JOURNAL OF MATERIALS SCIENCE 30 (1995) 4149–4154

Densification of acid-catalysed silica xerogels

K. DAHMOUCHE, C. BOVIER, J. DUMAS, J. SERUGHETTI
Département de physique des matériaux, UA CNRS 172, Université Claude Bernard, Lyon 1, 43 bd du 11 novembre 1918 69622 Villeurbanne, France

C. MAI
GEMPPM, UA CNRS 341, INSA de Lyon, 20 Avenue Albert Einstein 69622 Villeurbanne, France

Wet acid-catalysed gels prepared by hydrolysis and condensation of tetramethylorthosilicate (TMOS) can be dried without the occurrence of fractures or cracks when drying conditions are appropriate. Furthermore, the resultant dried gel monoliths can be converted to silica glass on heating to 1100 °C and holding there for 30 min when the composition of the starting solution is appropriate.

The xerogel to glass transformation was followed by scanning electron microscopy (SEM), small-angle X-ray scattering, Brunauer–Emmett–Teller (BET) measurements, low-frequency Raman scattering and dilatometric measurements and reveals that the densification process is different from the one described for base-catalysed xerogels.

1. Introduction

The most serious problems encountered in the sol–gel preparation of silica glass monoliths are crack formation or fracture [1] taking place in the process of drying wet gels, and crack formation and bloating [2] observed on heating to convert dried gels to silica glass.

This paper presents the process used to dry wet acid-catalysed gels without occurrence of fracture or cracks in the material, and describes the densification process, which allows the conversion of acid-catalysed xerogels to silica glass monoliths. Finally we compare this densification process with the one described for base-catalysed xerogels [3, 4].

2. Experimental procedure

2.1. Preparation of the starting solution, gelation and drying

Gels were prepared by hydrolysis and condensation of a solution of tetramethylorthosilicate (TMOS), oxalic acid and water. The sol was kept at 60 °C for 7 h. After gelation, the temperature was raised from 60 to 80 °C over 20 h and held at this temperature for 5 h in order to age the wet gel. Drying of the gel was conducted by perforating the aluminium foil covering the gel container. The temperature was increased to 150 °C over 70 h and held there for 24 h. After these operations a silica xerogel monolith without cracks or fracture was obtained (Fig. 1). This sample had a specific surface area of 632 $m^2 g^{-1}$, a pore volume of 0.44 $cm^3 g^{-1}$ and a micropore radius of about 0.7 nm, results given by Brunauer–Emmett–Teller (BET) measurements. The apparent density was 1.12 $g cm^{-3}$.

2.2. Sintering of the dried gels

The samples were sintered in an air atmosphere between 160 and 1100 °C. The temperature was raised at a rate of 18 °C h^{-1}. The samples were taken out of the furnace at different temperatures after annealing for 30 min and tested by various methods.

2.3. Characterization techniques

Fracture surfaces of Au 20% Pt coated gels were observed with an Hitachi type S-800 scanning electron microscope (SEM).

The small angle X-ray scattering (SAXS) measurements were performed by a high power rotating anode generator (12 kW) with a position sensitive detector. A multichannel analyser connected to a microcomputer allows fast measurements to be made. The X-ray beam of wavelength 0.154 nm ($CuK_{\alpha 1}$) is focused on the detector plane by a curved monochromator. The X-ray beam is held under vacuum in order to reduce air scattering. Point-like slit conditions with an irradiated cross-section of about 1 mm^2 are used.

The BET measurements were realized by the adsorption–desorption of nitrogen by the sample at very low temperature (−196 °C). The Raman measurements were obtained with a Dilor monochromator using the 514.5 nm line of an argon ion laser as an excitation source and a cooled photomultiplier. The range investigated varied from 3 to 700 cm^{-1}. The dilatometric measurements were performed with an Adamel D24 apparatus.

3. Results and discussion

Fig. 2(a) shows a SEM picture of the xerogel dried at 150 °C. It shows a granular microstructure consisting

0022–2461

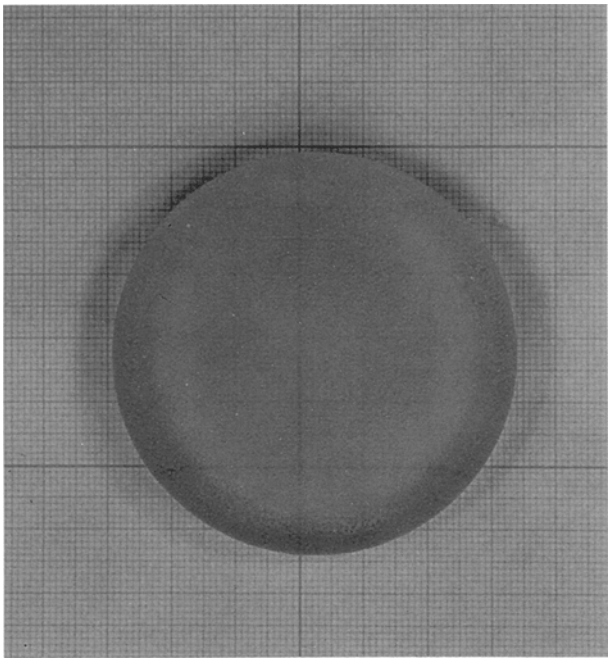

Figure 1 Image of the xerogel dried at 150 °C.

of clusters with a diameter between 10.0 and 50.0 nm constituted of particles (beads) with a diameter of about 5.0 nm. Fig. 2(b) and (c) show the SEM picture of this sample annealed for 30 min at 965 and 1020 °C. The clusters are also present but the particles inside disappear progressively with the increase of temperature. Fig. 2(d) shows the SEM picture of the sample annealed for 30 min at 1100 °C. It shows a non-porous uniform structure revealing that the xerogel has been converted to glass at this temperature.

The evolution of the texture of the xerogel with heat-treatment was also followed by SAXS: Fig. 3 shows the SAXS intensity in function of the scattering vector Q for xerogels annealed in air between 150 and 1020 °C. On the one hand the presence of a maximum located at 0.378 nm^{-1} for the sample dried at 150 °C (Fig. 3(a)) is observed. This peak is attributed to a correlation distance (about 16.5 nm) between particles or clusters in the xerogel. This allows to confirm the existence of the clusters observed by SEM, the value 16.5 nm also being the average size of these clusters. This figure shows a small shift of the peak corresponding to a small decrease of the correlation distance from 16.5 nm at 150 °C (a) to 13.5 nm at 700 °C (Fig. 3(b)). This shift is attributed to a small collapse of the texture of the xerogel which makes the clusters to approach each other in this domain of temperature. On the other hand the figure shows that the maximum is always present when the temperature increases (even at 1020 °C) confirming the SEM observations. Finally the position of the peak does not change between 700 °C (b) and 1020 °C (c) confirming the SEM observations, which showed no collapse of the texture of the xerogel in this domain of temperature but only a disappearance of the beads inside the clusters.

The sample annealed for 30 min at 1100 °C shows no X-ray scattering, confirming the transformation of the xerogel to glass at this temperature.

In order to complete our knowledge of the textural evolution of the material during the densification we studied the porosity by BET measurements. The results are given in Table I. The apparent density (d_a) is the density of the whole sample (pores + solid phase) while d_s is the density of the solid phase only which is obtained with the relation

$$V_p = 1/d_a - 1/d_s \quad (1)$$

where V_p is the total volume of the pores. This volume is the saturation value given by the adsorption–desorption

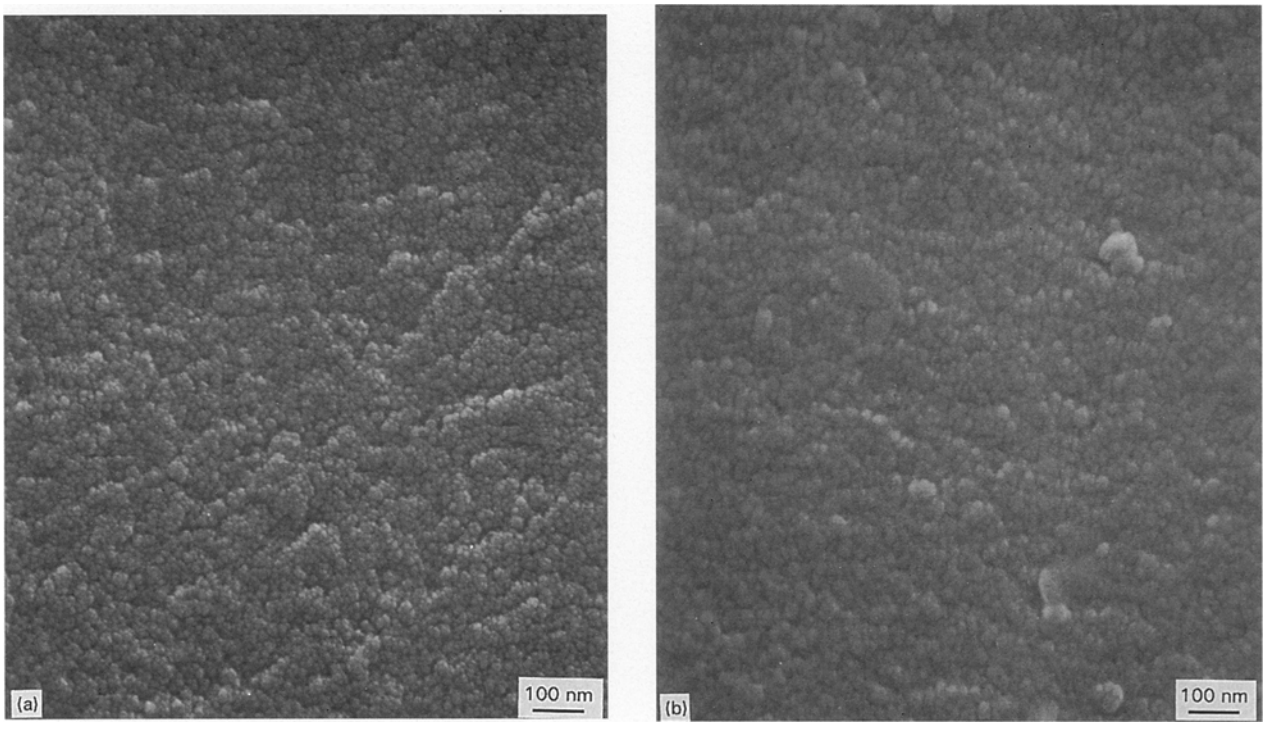

Figure 2 Scanning electron microscopy image of the xerogel: (a) dried at 150 °C, (b) annealed for 30 min at 965 °C, (c) annealed for 30 min at 1020 °C and (d) annealed for 30 min at 1100 °C.

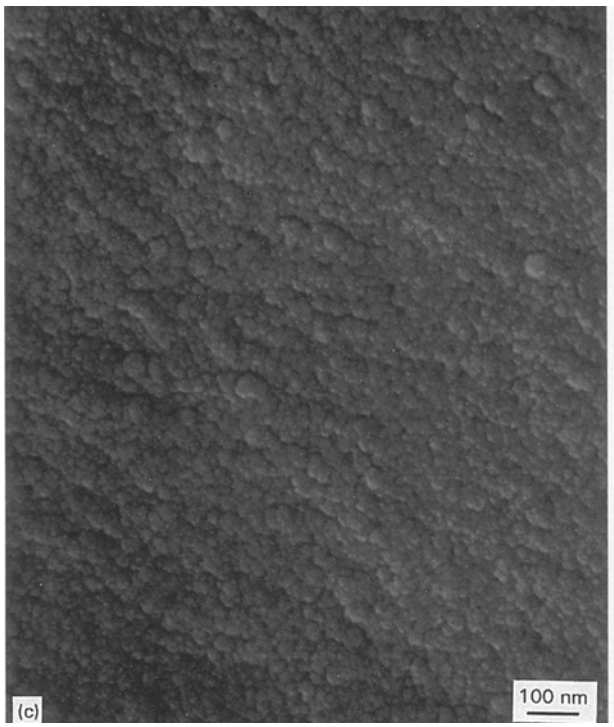

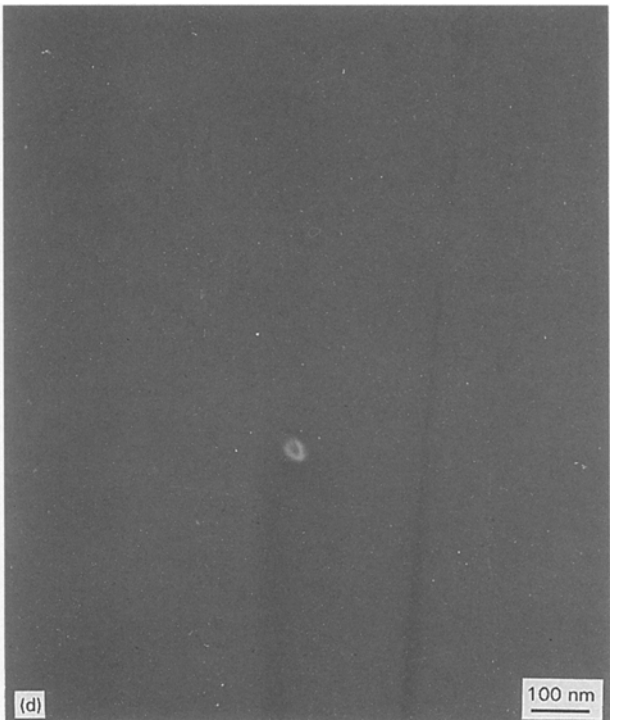

Figure 2 (continued)

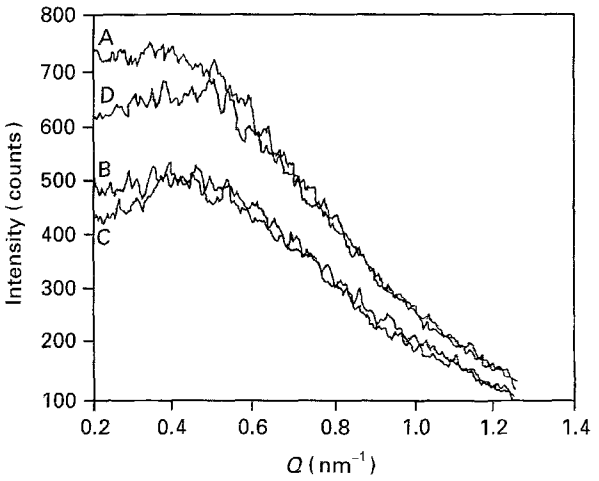

Figure 3 SAXS intensity in function of the scattering vector Q from acid-catalysed xerogels: (a) dried at 150 °C; (b) annealed for 30 min at 700 °C; (c) annealed for 30 min at 965 °C; (d) annealed for 30 min at 1020 °C. The time for the SAXS experiment was 7200 s.

TABLE I Evolution of the apparent density (d_a), the pore volume (V_p), the specific surface area (S) and the micropore radius (nm) as a function of temperature for the acid-catalysed xerogel.

	150 °C	700 °C	965 °C	1020 °C	1100 °C
Apparent density d_a ($g\,cm^{-3}$)	1.12	1.16	1.34	1.55	2.2
Pore volume V_p ($cm^3\,g^{-1}$)	0.44	0.41	0.29	0.19	0
Specific surface area S ($m^2\,g^{-1}$)	632	600	488	254	0
Micropore radius (nm)	0.7	0.7	0.7	0.7	0

isotherm of nitrogen by the sample (adsorbed nitrogen volume as a function of the relative pressure). The micropore radius is obtained by the "t" method [5]. The variation analysis of the slope of the "t" straight line allows us to know the lower and upper limit of the micropore size. The value of d_s is about 2.2 $g\,cm^{-3}$ at each temperature, showing that the solid phase has the density of vitreous silica.

During the process of densification the micropore radius is always about 0.7 nm showing that it is the number of the micropores which decreases and contributes to the diminishing pore volume. This decrease of the porosity is divided into two temperature ranges. The first is 150–700 °C and shows a very small evolution of d_a, V_p and S. This domain corresponds to the small collapse of the texture of the material observed by SAXS and to the beginning of the process of disappearance of the beads inside the clusters observed by SEM. The second range, 700–1100 °C, shows a great evolution of d_a, V_p and S, whose values reach, at 1100 °C, those of the vitreous silica. This domain corresponds to the disappearance of the beads inside the clusters (700–1020 °C) and then of the clusters themselves (1020–1100 °C), phenomena observed by SAXS and SEM.

In order to have information about the structural evolution of the xerogel during the densification we performed Raman scattering experiments: Fig. 4 shows the reduced Raman spectra $I(\omega)/(n(\omega)+1)$ (where $I(\omega)$ is the Raman intensity, ω the frequency and $n(\omega)$ the Bose factor) up to 200 cm^{-1} for xerogels annealed between 150 and 1100 °C for 30 min. At first, we can see the presence of a very low frequency band located at 23 cm^{-1} for the sample dried at 150 °C (Fig. 4 (a)). This kind of peak has already been observed with base-catalysed aerogels [6] and base-catalysed xerogels [3] and can be attributed to surface-vibrational modes of particles which are aggregated to form the gel. This result confirms that the structure inside

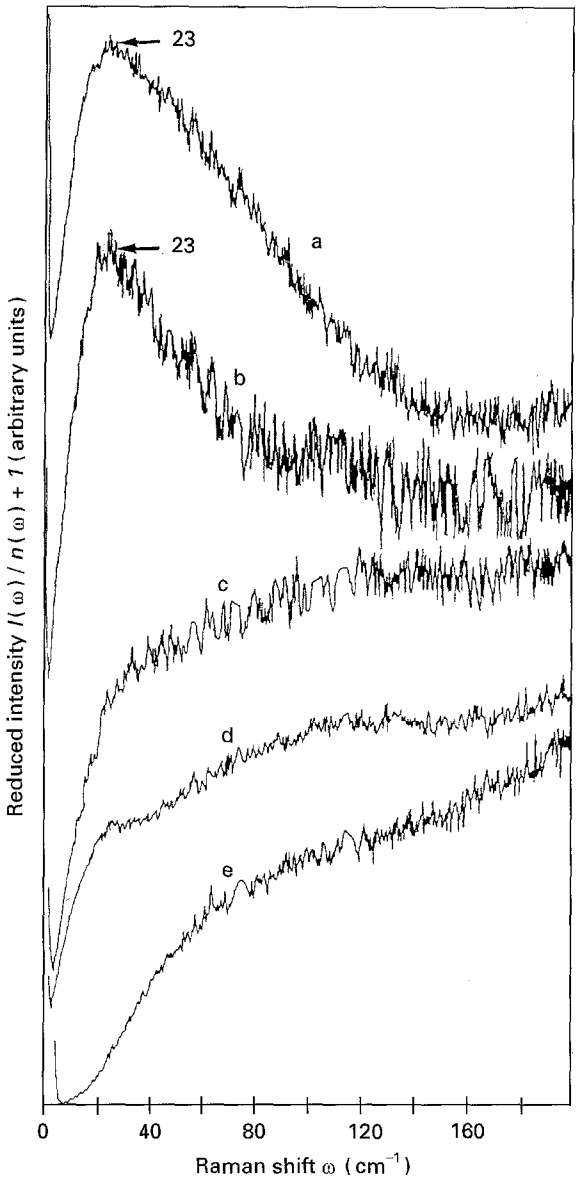

Figure 4 Low-frequency Raman reduced intensity from acid-catalysed xerogels: (a) dried at 150 °C; (b) annealed for 30 min at 700 °C; (c) annealed for 30 min at 965 °C; (d) annealed for 30 min at 1020 °C; (e) annealed for 30 min at 1100 °C.

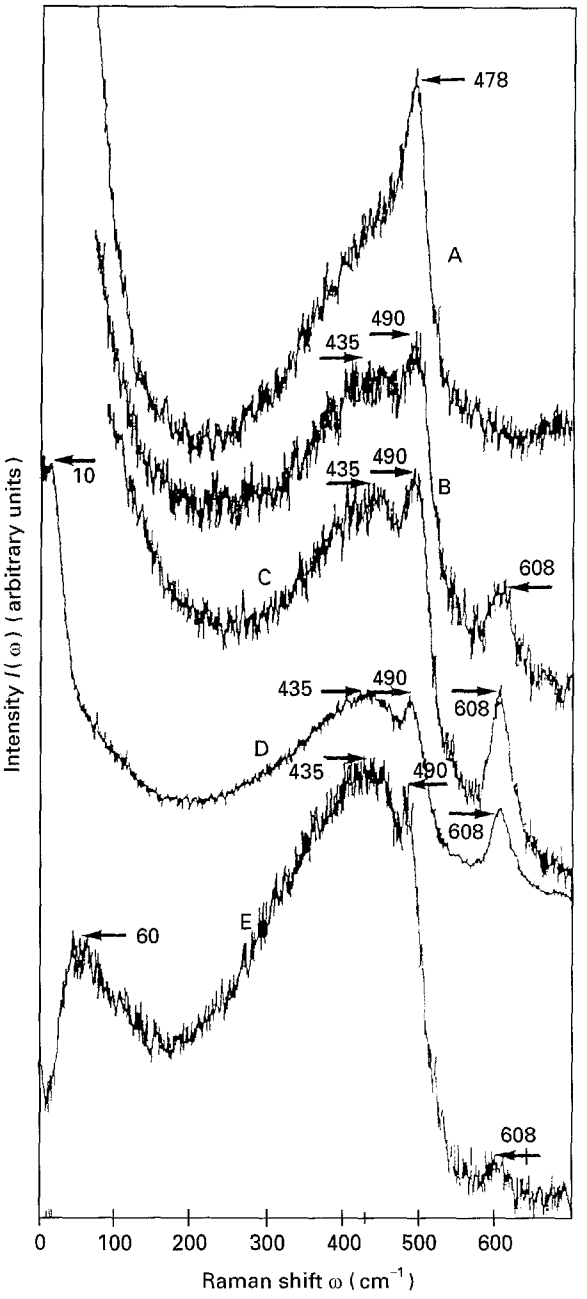

Figure 5 Raman intensity from acid-catalysed xerogels: (a–e) same samples as in Fig. 4.

the clusters observed by SEM is constituted of particles (beads). On the other hand, the frequency ω_0 of the maximum is a function [7] of the sound velocity v in the particle, of the light velocity c in vacuum and of the diameter $2a$: $\omega_0 = 0.8\ (v/2ac)$. Choosing a velocity $v = 4000\ m\ s^{-1}$, value slightly smaller than in silica, it is found to be $2a = 4.5$ nm, the size of the beads. Finally, the spectrum of the sample annealed for 30 min at 700 °C (Fig. 4(b)) shows no modification of the position of the peak but the spectrum of the sample annealed for 30 min at 965 °C (Fig. 4(c)) shows that the maximum disappeared, revealing that the particles (beads) are not individualized at this temperature. This confirms the progressive disappearance of these particles inside the clusters (which are always present up to 1020 °C) with the increase of temperature, a phenomenon observed by SEM. The spectrum of the sample annealed for 30 min at 1020 °C (Fig. 4(d)) shows the evolution of the structure of the gel in order to reach the fused silica one at 1100 °C (Fig. 4(e)).

It is interesting to consider Raman scattering at higher frequencies, due to the vibrational modes inside the particles. In fig. 5 the direct spectra up to 700 cm^{-1} for the different previous heat-treatments are presented. We can see the appearance of the broad band (located at 435 cm^{-1}) of the silica at 700 °C Fig. 5(b) which does not exist at 150 °C (a). This band is characteristic of the disorder at short distance and this evolution shows a modification of the internal structure of the particles between 150 and 700 °C. On the other hand, the appearance of the line at 608 cm^{-1} (which corresponds to a 3-fold planar ring formed from three tetrahedra [8]) for the sample heat-treated at 700 °C reflects the modification of the surface of the particles. The surface which was rough becomes smooth [9].

The comparison of these two spectra also shows that the line at 478 cm^{-1} observed in Fig. 5(a) shifts to about 490 cm^{-1} in Fig. 5(b). These lines at 478 and 490 cm^{-1}

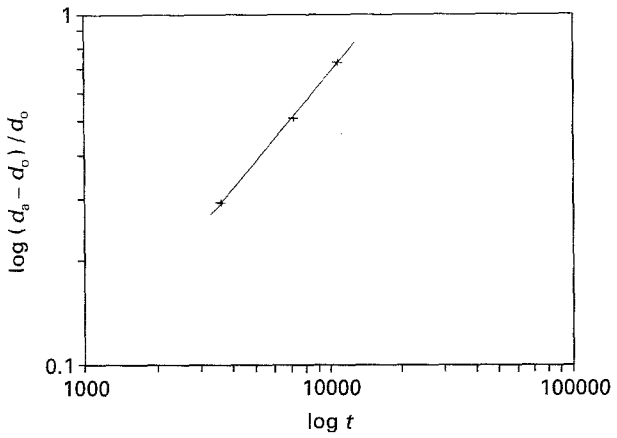

Figure 6 Log–log plot of $(d_a–d_0)/d_0$ versus t at 700 °C.

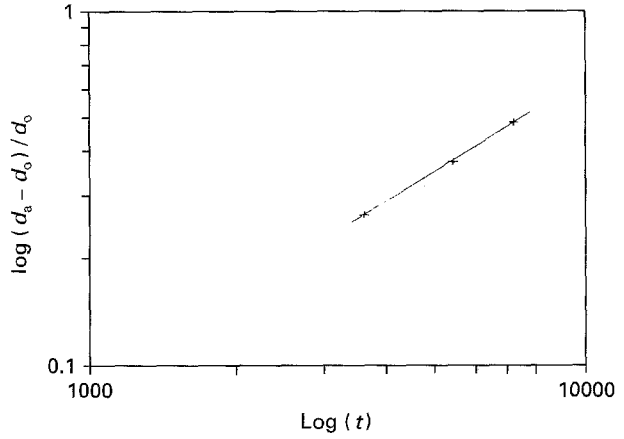

Figure 7 Log–log plot of $(d_a–d_0)/d_0$ versus t at 965 °C.

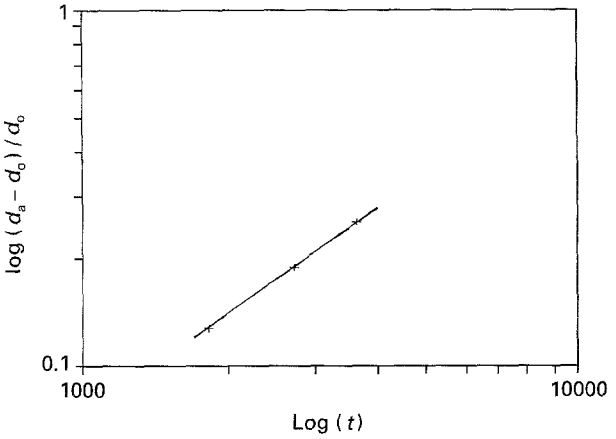

Figure 8 Log–log plot of $(d_a–d_0)/d_0$ versus t at 1020 °C.

TABLE II Dilatometric measurements as a function of annealing time for the acid-catalysed xerogel

Temperature (°C)	Annealing time	Apparent density d_a (g cm^{-3})
700	30 min ($t = 0$)	1.16
	1.5 h ($t = 1$ h)	1.5
	2.5 h ($t = 2$ h)	1.75
	3.5 h ($t = 3$ h)	2
965	30 min	1.34
	1.5 h	1.7
	2 h	1.85
	2.5 h	2
1020	30 min	1.55
	1 h	1.75
	1.25 h	1.85
	1.5 h	1.9

can be assigned to the 4-fold planar ring, respectively at the surface and inside the particles [10]. This shift reflects again the modification of the silica particles from rough to smooth. The comparison between Fig. 5(b), (c), (d) and (e) reveals that the line due to the 4-fold planar ring (located about 490 cm^{-1}) increases compared to the line due to the 3-fold planar ring (located about 608 cm^{-1}). It shows the progressive evolution of the structure of the xerogel to the glass with the increase of temperature, also reflected by the increase of the intensity of the broad band (located at 435 cm^{-1}) compared to the line about 490 cm^{-1} and by the apparition of an incipient boson peak (located at 10 cm^{-1}) at 1020 °C (Fig. 5(d)). At 1100 °C the spectrum is similar to the fused silica one (Fig. 5(e)).

Much information is now available about the evolution of the texture and the structure of the acid-catalysed xerogel with heat-treatment, but what is the mechanism responsible for the disappearance of the particles inside the clusters? In order to answer this question we performed dilatometric measurements.

Figs 6, 7 and 8 show log–log plots of $(d_a - d_0)/d_0$ versus t (time of annealing), where d_0 is the apparent density of the xerogel when $t = 0$. This origin $t = 0$ is taken for a real heat-treatment of 30 min. The results are also given in Table II. The three temperatures show a linear variation meaning that $(d_a - d_0)/d_0 = Kt^m$: for $T = 700$ °C $m = 0.82$; for $T = 965$ °C $m = 0.88$; for $T = 1020$ °C $m = 1$. Those exponents near 1 are characteristic of a densification by viscous sintering [11].

The disappearance of the beads is thus due to a viscous sintering mechanism. As showed by SEM, this mechanism is progressive and continuous. The number of the pores decreases progressively when the temperature increases (see BET measurements) in order to reach the non-porous texture of the vitreous silica at 1100 °C.

All these results show that the densification process for acid-catalysed xerogels consists of two stages: the first is a small collapse of the clusters (between 150 and 700 °C) and the second is the disappearance of the beads and of the porosity by a viscous sintering mechanism in order to reach the non-porous texture of a silica glass at 1100 °C.

It is thus interesting to compare the densification process between acid- and base-catalysed xerogels which has been described in recent papers [3, 4]. The textural characteristic of the dried gels (not heat-treated) are very different, although they are both formed by clusters of size between 10.0 and 50.0 nm constituted of beads of diameter about 5.0 nm.

The most important point is that the densification process concerning the textural evolution of the xerogel is very different as is illustrated by comparing Figs 4 and 9 [3] which represent the reduced Raman

TABLE III Comparison of the texture of the acid and base-catalyzed dried gels.

	Apparent density ($g\,cm^{-3}$)	Pore volume ($cm^3\,g^{-1}$)	Specific surface area ($m^2\,g^{-1}$)	pore radius (nm)
Acid-catalysed gel (dried to 150 °C)	1.12	0.44	632	0.7
Base-catalysed gel (dried to 160 °C)	0.54	1.2	617	4.3

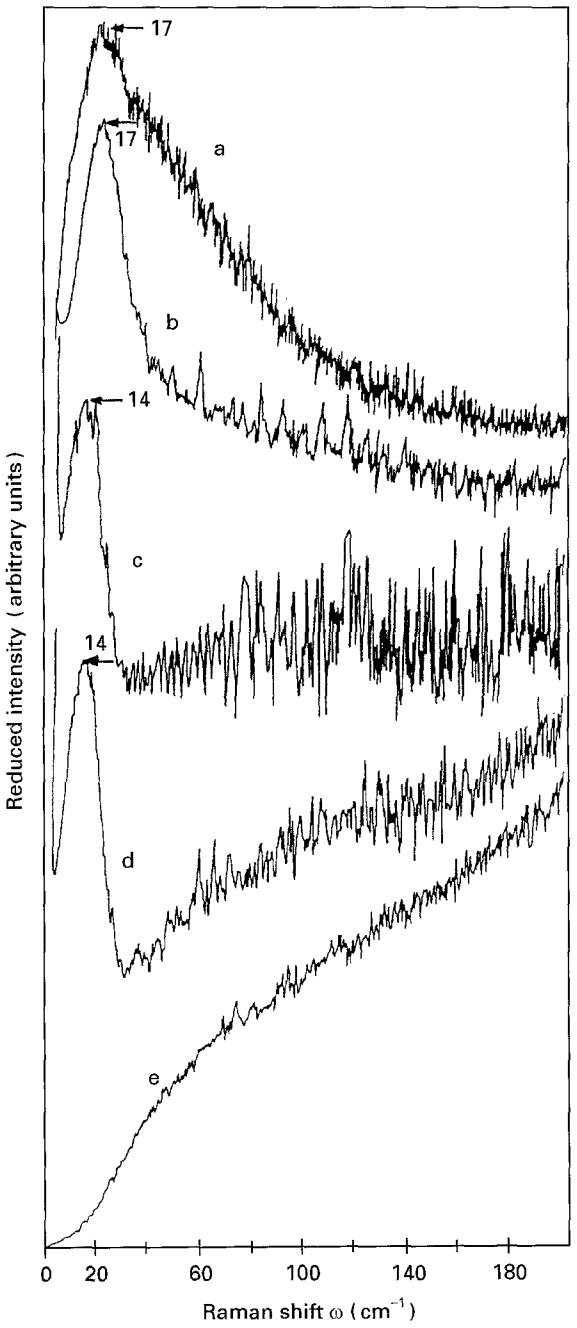

Figure 9 Low-frequency Raman reduced intensity from base-catalysed xerogels: (a) dried at 160 °C; (b) annealed for 30 min at 700 °C; (c) annealed for 30 min at 980 °C; (d) annealed for 30 min at 1030 °C; (e) annealed for 30 min at 1050 °C.

spectra $I(\omega)/(n(\omega)+1)$ up to 200 cm^{-1}, respectively, for acid and base-catalysed xerogels annealed up to the temperature of conversion to silica glass. In Fig. 4 the spectrum of the sample annealed for 30 min at 965 °C (Fig. 4(c)) shows that the maximum attributed to vibrational modes of particles (beads) disappeared but in Fig. 9 the spectrum of the sample annealed for 30 min at 980 °C (Fig. 9(c)) shows that this maximum is present. Both samples are porous (pore volume about 0.29 $cm^3\,g^{-1}$ for the acid-catalysed xerogel and 0.6 $cm^3\,g^{-1}$ for the base-catalysed one [3, 4]) so are not converted to glass. This illustrates the main difference between the two densification processes: for acid-catalysed xerogel the elimination of the particles inside the clusters by viscous sintering between 700 and 1020 °C (so the maximum disappears at 965 °C) happens before the elimination of the clusters themselves between 1020 and 1100 °C which is the temperature of conversion to glass. For base-catalyzed xerogels, however, the evolution of the texture consists of a strong collapse of the clusters about 980 °C [4] although the particles are ever-present (the maximum is present at 980 °C). Then a second phenomenon, which is probably simultaneous to the previous one, happens at temperature higher than 1030 °C and consists of a sintering of the beads in order to reach the non-porous structure of a silica glass at 1050 °C [3, 4].

4. Conclusions

SEM, BET and dilatometric measurements, small-angle X-ray scattering and low-frequency Raman scattering allows the process of densification of acid-catalysed xerogels to be described. Several stages can be distinguished: small collapse of the clusters, smoothing of the particles (beads) constituting the clusters and elimination of these particles by viscous sintering. A continuous evolution of the structure at short distances (inside particles) is also observed in order to reach the structure of fused silica at 1100 °C.

References

1. J. ZARZYCKI in "Ultrastructure processing of ceramics, glasses and composites" edited by L. Hench and D. R. Ulrich (Wiley, New York, 1984) p. 27.
2. T. KAWAGUCHI, H. HISHIKURA, J. IURA and Y. KOKUBU, *J. Non-Cryst. Solids* **63** (1984) 61.
3. K. DAHMOUCHE, A. BOUKENTER, C. BOVIER, J. DUMAS, E. DUVAL and J. SERUGHETTI, *Ibid.* **147, 148** (1992) 251.
4. K. DAHMOUCHE, C. BOVIER, A. BOUKENTER, J. DUMAS, E. DUVAL, C. MAI and J. SERUGHETTI, Journal de physique IV Colloque C2, supplément au journal de physique III volume 2 (1992) 127.
5. S. BRUNAUER, R. S. MIKHAIL and E. E. BODOR, *J. Colloid Interface Sci.* **26** (1968) 45.
6. A. BOUKENTER, B. CHAMPAGNON, E. DUVAL, J. L. ROUSSET, J. DUMAS and J. SERUGHETTI, *J. Phys. C: Solid State Phys.* **21** (1988) 1097.
7. E. DUVAL, A. BOUKENTER and B. CHAMPAGNON, *Phys. Rev. Lett.* **56** (1986) 2052.
8. FI. GALEENER, *Solid. State Commun.* **44** (1982) 1037.
9. R. VACHER, T. WOIGNIER, J. PELOUS and E. COURTENS, *Phys. Rev. B.* **37** (1988) 6500.
10. G. E. WALRAFEN, M. S. HOKMAMADI and N. C. HOLMES, *J. Chem. Phys.* **85** (1986) 771.
11. J. FRENKEL, *J. Phys. (Moscow)* **5** (1945) 385.

Received 11 April 1994
and accepted 3 February 1995